Plane wave prediction in 3-D[a]

[a]Published in SEP report, 102, 101-110 (1999)

Sergey Fomel[1]

INTRODUCTION

The theory of plane-wave prediction in three dimensions is described by Claerbout (1993, 1999). Predicting a local plane wave with T-X filters amounts to finding a pair of two-dimensional filters for two orthogonal planes in the 3-D space. Each of the filters predicts locally straight lines in the corresponding plane. The system of two 2-D filters is sufficient for predicting all but purely vertical plane waves. In the latter case, a third 2-D filter for the remaining orthogonal plane is needed. Schwab (1998) discusses this approach in more detail.

Using two prediction filters implies dealing with two filtering output volumes for each input volume. This situation becomes inconvenient when one uses the prediction output as a measure of coherency in the input volume (Claerbout, 1993; Schwab et al., 1996). Two outputs are obviously more difficult to interpret than one, and there is no natural way of combining them into one image. Another difficulty arises when plane-wave destructors are used for regularizing linear inverse problems (Clapp et al., 1997). We cannot apply an efficient recursive preconditioning (Claerbout, 1998a) unless the regularization operator is square, or, in other words, only one plane-wave destructor is involved.

Helical filtering (Claerbout, 1998b) brings us new tools for addressing this problem. In this paper, I show how to combine orthogonal 2-D plane predictors into a single three-dimensional filter with similar spectral properties. The 3-D filter can then work for coherency measurements or for preconditioning 3-D inverse problems. The construction employs the Wilson-Burg method of spectral factorization, adapted for multidimensional filtering with the help of the helix transform (Sava et al., 1998).

I use simple synthetic examples to demonstrate the applicability of plane-wave prediction to 3-D problems.

FACTORIZING PLANE WAVES

Let us denote the coordinates of a three-dimensional space by t, x, and y. A theoretical plane wave is described by the equation

$$U(t,x,y) = f(t - p_x x - p_y y) \;, \tag{1}$$

where f is an arbitrary function, and p_x and p_y are the plane slopes in the corresponding direction. It is easy to verify that a plane wave of the form (1) satisfies the following system

[1]**e-mail:** sergey@sep.stanford.edu

of partial differential equations:

$$\left\{ \begin{array}{rcl} \left(\dfrac{\partial}{\partial x} + p_x \dfrac{\partial}{\partial t} \right) U &=& 0 \\ \left(\dfrac{\partial}{\partial y} + p_y \dfrac{\partial}{\partial t} \right) U &=& 0 \end{array} \right. \tag{2}$$

The first equation in (2) describes plane waves on the $\{t, x\}$ slices. In is discrete form, it is represented as a convolution with the two-dimensional finite-difference filter $\mathbf{A}_x$. Similarly, the second equation transforms into a convolution with filter $\mathbf{A}_y$, which acts on the $\{t, y\}$ slices. The discrete (finite-difference) form of equations (2) involves a blocked convolution operator:

$$\left(\begin{array}{c} \mathbf{A}_x \\ \mathbf{A}_y \end{array} \right) \mathbf{U} = \mathbf{0} \; . \tag{3}$$

where $\mathbf{U}$ is the model vector corresponding to $U(t, x, y)$.

In many applications, we are actually interested in the spectrum of the prediction filter, which approximates the inverse spectrum of the predicted data. In other words, we deal with the square operator

$$\left(\begin{array}{cc} \mathbf{A}_x^T & \mathbf{A}_y^T \end{array} \right) \left(\begin{array}{c} \mathbf{A}_x \\ \mathbf{A}_y \end{array} \right) = \mathbf{A}_x^T \mathbf{A}_x + \mathbf{A}_y^T \mathbf{A}_y \; . \tag{4}$$

If we were able to transform this operator to the form $\mathbf{A}^T \mathbf{A}$, where $\mathbf{A}$ is a three-dimensional minimum-phase convolution, we could use the three-dimensional filter $\mathbf{A}$ in place of the inconvenient pair of $\mathbf{A}_x$ and $\mathbf{A}_y$.

The problem of finding $\mathbf{A}$ from its spectrum is known as spectral factorization. It is well understood for 1-D signals (Claerbout, 1976), but until recently it was an open problem in the multidimensional case. Helix transform maps multidimensional filters to 1-D by applying special boundary conditions and allows us to use the full arsenal of 1-D methods, including spectral factorization, on multidimensional problems (Claerbout, 1998b). A problem, analogous to (4), has already occurred in the factorization of the discrete two-dimensional Laplacian operator:

$$\Delta = \nabla^T \nabla = \left(\begin{array}{cc} \mathbf{D}_x^T & \mathbf{D}_y^T \end{array} \right) \left(\begin{array}{c} \mathbf{D}_x \\ \mathbf{D}_y \end{array} \right) = \mathbf{H}^T \mathbf{H} \; , \tag{5}$$

where $\mathbf{D}_x$ and $\mathbf{D}_y$ represent the partial derivative operators along the x and y dimensions, respectively, and the two-dimensional filter $\mathbf{H}$ has been named *helix derivative* (Claerbout, 1999; Zhao, 1999).

If we represent the filter $\mathbf{A}_x$ with the help of a simple first-order upwind finite-difference scheme

$$\mathbf{U}_{x+1}^t - \mathbf{U}_x^t + p_x \left(\mathbf{U}_{x+1}^{t+1} - \mathbf{U}_{x+1}^t \right) = 0 \; , \tag{6}$$

then, after the helical mapping to 1-D, it becomes a one-dimensional filter with the Z-transform

$$\mathbf{A}_x(Z) = 1 - p_x Z^{N_t+1} + (p_x - 1) Z^{N_t} \; , \tag{7}$$

where N_t is the number of samples on the t-axis. Similarly, the filter $\mathbf{A}_y$ takes the form

$$\mathbf{A}_y(Z) = 1 - p_y Z^{N_t N_x + 1} + (p_y - 1) Z^{N_t N_x} \ . \tag{8}$$

The problem is reduced to a 1-D spectral factorization of

$$\begin{aligned} \mathbf{A}_x(1/Z)\mathbf{A}_x(Z) + \mathbf{A}_y(1/Z)\mathbf{A}_y(Z) = & -p_y \tfrac{1}{Z^{N_t N_x + 1}} + (p_y - 1)\tfrac{1}{Z^{N_t N_x}} - \\ & p_x \tfrac{1}{Z^{N_t + 1}} + (p_x - 1)\tfrac{1}{Z^{N_t - 1}} + [p_x(1 - p_x) + p_y(1 - p_y)]\ \tfrac{1}{Z} + \\ & 2 + p_x(p_x - 1) + p_y(p_y - 1) + [p_x(1 - p_x) + p_y(1 - p_y)]\ Z + \\ & (p_x - 1) Z^{N_t - 1} - p_x Z^{N_t + 1} + (p_y - 1) Z^{N_t N_x} - p_y Z^{N_t N_x + 1} \ . \end{aligned} \tag{9}$$

After a minimum-phase factor of (9) has been found, we can use it for 3-D forward and inverse convolution.

All examples in this paper actually use a slightly more sophisticated formula for 2-D plane-wave predictors:

$$\mathbf{A}_x(Z) = 1 + \frac{p_x}{2}(1 - p_x) Z^{N_t - 1} + (p_x^2 - 1) Z^{N_t} - \frac{p_x}{2}(1 + p_x) Z^{N_t + 1} \ . \tag{10}$$

Formula (10) corresponds to the Lax-Wendroff finite difference scheme (Clapp et al., 1997). It provides a valid approximation of the plane-wave differential equation for $-1 \le p_x \le 1$.

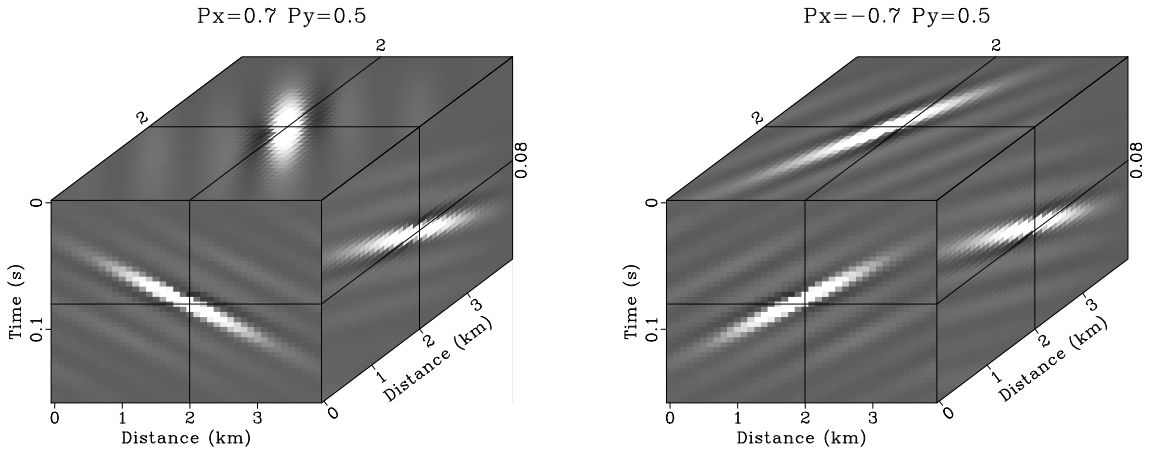

Figure 1: 3-D plane wave prediction with a 402-point filter. Left: $p_x = 0.7$, $p_y = 0.5$. Right: $p_x = -0.7$, $p_y = 0.5$.

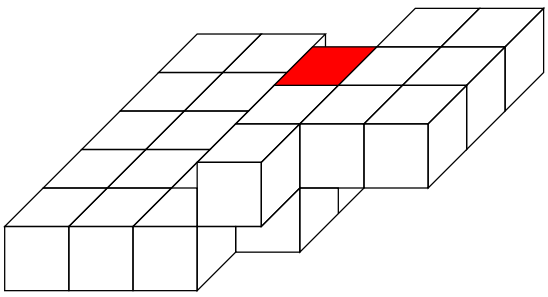

Figure 2: Schematic filter shape for a 26-point 3-D plane prediction filter. The dark block represents the leading coefficient. There are 9 blocks in the first row and 17 blocks in the second row.

Figure 1 shows examples of plane-wave construction. The two plots in the figure are outputs of a spike, divided recursively (on a helix) by $\mathbf{A}^T\mathbf{A}$, where $\mathbf{A}$ is a 3-D minimum-phase filter, obtained by Wilson-Burg factorization. The factorization was carried out in

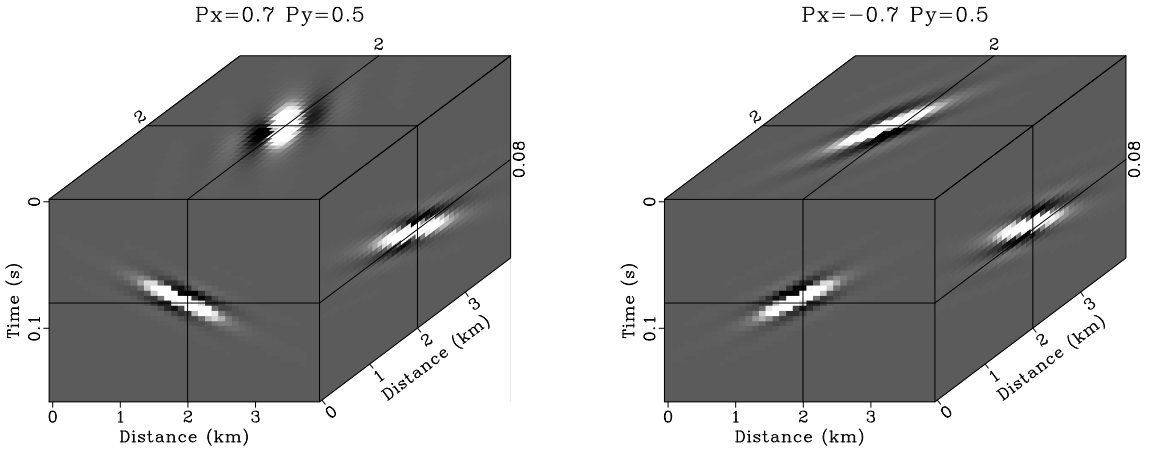

Figure 3: 3-D plane wave prediction with a 26-point filter. Left: $p_x = 0.7$, $p_y = 0.5$. Right: $p_x = -0.7$, $p_y = 0.5$.

the assumption of $N_t = 20$ and $N_x = 20$; therefore, the filter had $N_t N_x + 2 = 402$ coefficients. Using such a long filter may be too expensive for practical purposes. Fortunately, the Wilson-Burg method allows us to specify the filter length and shape beforehand. By experimenting with different filter shapes, I found that a reasonable accuracy can be achieved with a 26-point filter, depicted in Figure 2. Plane-wave construction for a shortened filter is shown in Figure 3. The predicted plane wave is shorter and looks more like a slanted disk. It is advantageous to deal with short plane waves if the filter is applied for local prediction of non-stationary signals.

Clapp (2000) has proposed constructing 3-D plane-wave destruction (steering) filters by splitting. In Clapp's method, the two orthogonal 2-D filters $\mathbf{A}_x$ and $\mathbf{A}_y$ are simply convolved with each other instead of forming the autocorrelation (4). While being a much more efficient approach, splitting suffers from induced anisotropy in the inverse impulse response. Figure 4 illustrates this effect in the 2-D plane by comparing the inverse impulse responses of plane-wave filters obtained by spectral factorization and splitting. The splitting response is evidently much less isotropic.

In the next sections, I address the problem of estimating plane-wave slopes and show some examples of applying local plane-wave prediction in 3-D problems.

ESTIMATING PLANE WAVES

It may seem difficult to estimate the plane slope p_x for a Lax-Wendroff filter of the form (10) because p_x appears non-linearly in the filter coefficients. However, using the analytical form of the filter, we can easily linearize it with respect to the plane slope and set up a simple iterative scheme:

$$p_x^{(k+1)} = p_x^{(k)} + \Delta p_x^{(k)} \ , \tag{11}$$

where k stands for the iteration count, and $\Delta p_x^{(k)}$ is found from the linearized equation

$$(\mathbf{A'}_x \mathbf{U})\, \Delta p_x = -\mathbf{A}_x \mathbf{U} \ , \tag{12}$$

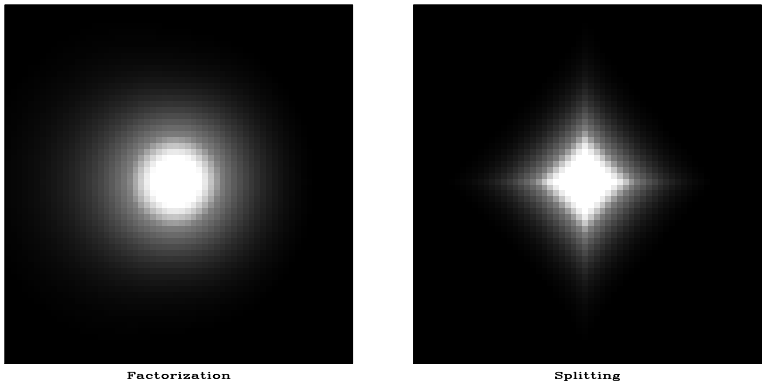

Figure 4: Two-dimensional inverse impulse responses for filters constructed with spectral factorization (left) and splitting (right). The splitting response is evidently much less isotropic.

where $\mathbf{A'}_x$ is the derivative of $\mathbf{A}_x$ with respect to p_x. To avoid unstable division by zero when solving equation (12) for Δp_x, Adding a regularization equation

$$\epsilon \nabla \Delta p_x \approx 0 \ , \tag{13}$$

where ϵ is a small scalar regularization parameter, I solve system (12-13) in the least-square sense to obtain a smooth slope variation Δp_x at each iteration. In practice, iteration process (11) quickly converges to a stable estimate of p_x.

EXAMPLES

Two simple examples in this section demonstrate an application of 3-D local plane-wave prediction to the problems of discontinuity enhancement and missing data interpolation.

3-D discontinuity enhancement

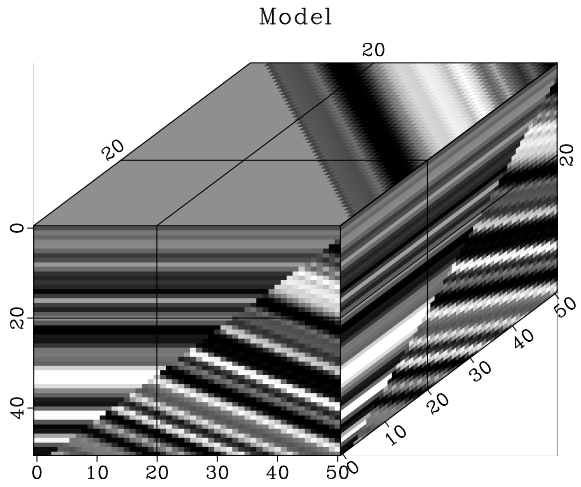

Figure 5: A synthetic model, showing a fault between two plane waves of different slopes.

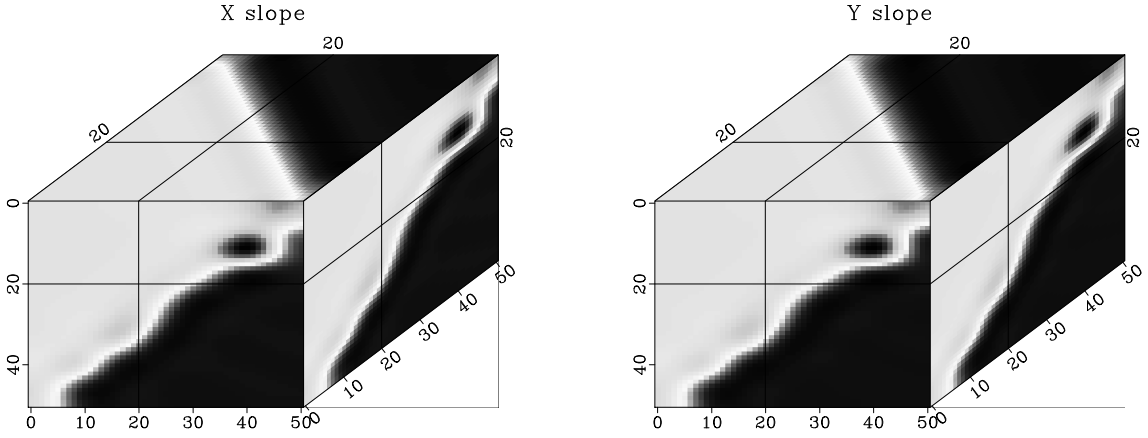

Figure 6: Plane wave slope estimates in the x and y directions (left and right plots, respectively) from the synthetic two-plane model.

Figure 5 shows a simple synthetic model of two plane waves, separated by a plane fault. The slope estimates for the two orthogonal directions are shown in Figure 6. We can see that the estimation procedure correctly identified the regions of constant slope. Finally, estimating a local 3-D plane-wave predictor by spectral factorization and convolving the resultant non-stationary filter with the input model, we obtain the prediction residual, shown in Figure 7. In the residual, both plane waves are effectively destroyed, and we observe a sharp image of the fault plane. This result compares favorably with results of alternative methods, collected by (Schwab, 1998).

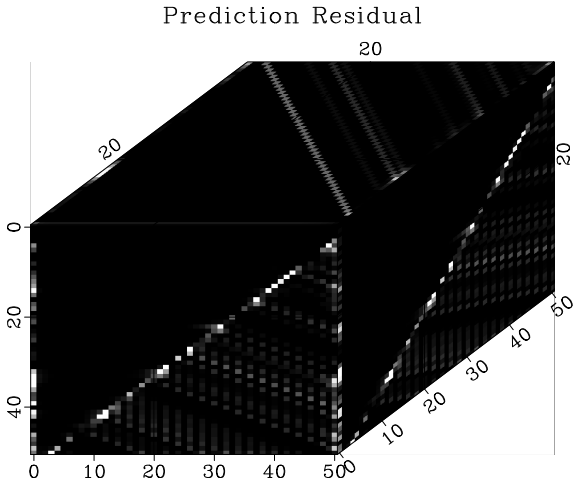

Figure 7: Magnitude of the residual after convolving the synthetic two-plane model with a local 3-D plane wave filter.

3-D missing data interpolation

Figures 8 and 9 show Claerbout's "qdome" synthetic model (Claerbout, 1993, 1999) and its corresponding slope estimates. In a missing data interpolation experiment, I remove 75% of the traces in the original model, arriving at the missing data model, shown in the left plot of Figure 10. The missing data interpolation result is shown in the right plot of Figure 10.

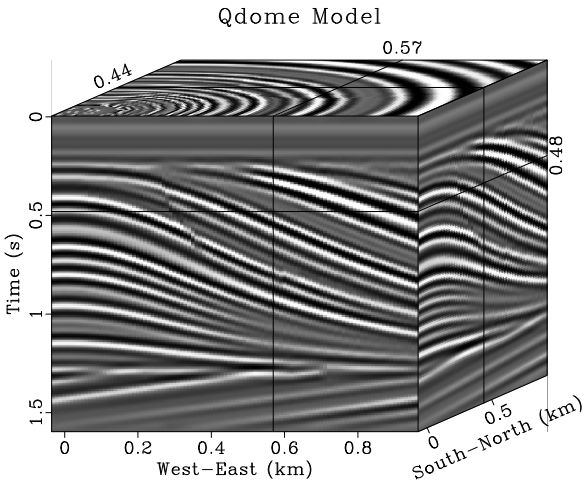

Figure 8: Claerbout's "qdome" synthetic model.

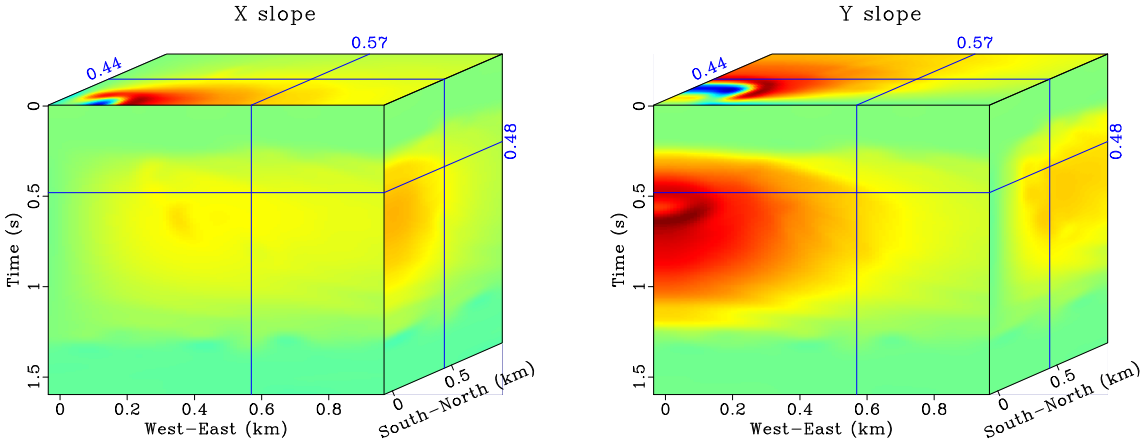

Figure 9: Plane wave slope estimates in the x and y directions (left and right plots, respectively) from the "qdome" model.

Most of the original signal, except for some high-curvature areas, has been restored. Local 3-D plane-wave predictors allow us to use the efficient interpolation technique of Fomel et al. (1997), based on recursive filter preconditioning.

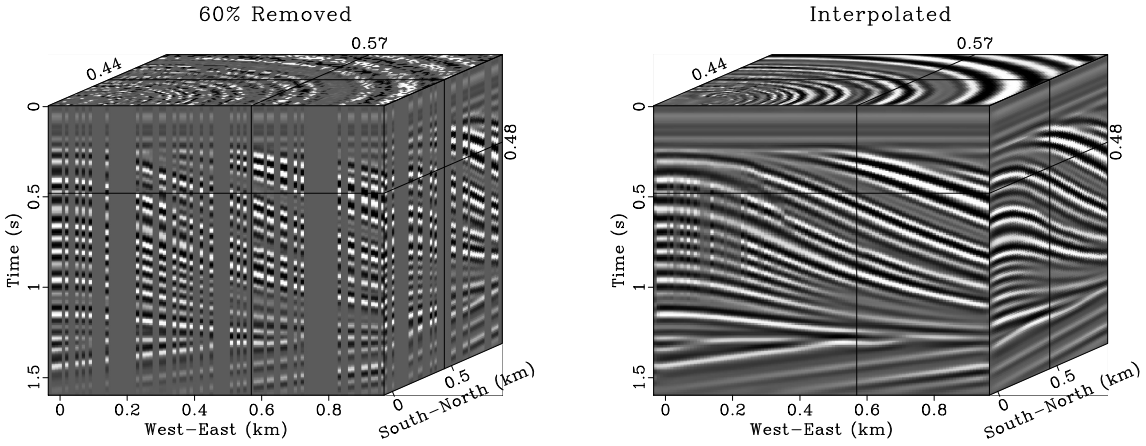

Figure 10: Left: "qdome" model with 75% of the randomly chosen traces removed. Right: result of missing data interpolation with a 3-D local plane-wave prediction filter.

CONCLUSIONS

I have shown that a 3-D plane-wave prediction filter can be constructed from a pair of two-dimensional filters by using helix transform and a one-dimensional spectral factorization algorithm.

In all the examples, I used analytical finite-difference filters instead of more general prediction-error filters. A similar factorization idea could be applied to 3-D prediction-error filters. However, treating non-stationarity in this case is less straightforward and requires additional care (Crawley et al., 1998; Clapp et al., 1999).

3-D plane-wave prediction filters can find many interesting applications in data processing and inversion. An especially promising application is solution steering in tomography-type problems (Clapp et al., 1997; Clapp and Biondi, 1998).

ACKNOWLEDGMENTS

Jon Claerbout suggested the problem of 3-D plane wave prediction and the idea of its solution. Unfortunately, he is currently not able to share the authorship.

REFERENCES

Claerbout, J., 1998a, Multidimensional recursive filters via a helix, *in* SEP-97: Stanford Exploration Project, 319–335.

———, 1998b, Multidimensional recursive filters via a helix: Geophysics, **63**, 1532–1541.

———, 1999, Geophysical estimation by example: Environmental soundings image enhancement: Stanford Exploration Project.

Claerbout, J. F., 1976, Fundamentals of geophysical data processing: Blackwell.

———, 1993, 3-D local monoplane annihilator, *in* SEP-77: Stanford Exploration Project, 19–25.

Clapp, R., 2000, 3-D steering filters, *in* SEP-105: Stanford Exploration Project, 109–116.

Clapp, R. G., and B. L. Biondi, 1998, Regularizing time tomography with steering filters, *in* SEP-97: Stanford Exploration Project, 137–146.

Clapp, R. G., S. Fomel, and J. Claerbout, 1997, Solution steering with space-variant filters, *in* SEP-95: Stanford Exploration Project, 27–42.

Clapp, R. G., S. Fomel, S. Crawley, and J. F. Claerbout, 1999, Directional smoothing of non-stationary filters, *in* SEP-100: Stanford Exploration Project, 197–209.

Crawley, S., R. Clapp, and J. Claerbout, 1998, Decon and interpolation with nonstationary filters, *in* SEP-97: Stanford Exploration Project, 183–192.

Fomel, S., R. Clapp, and J. Claerbout, 1997, Missing data interpolation by recursive filter preconditioning, *in* SEP-95: Stanford Exploration Project, 15–25.

Sava, P., J. Rickett, S. Fomel, and J. Claerbout, 1998, Wilson-Burg spectral factorization with application to helix filtering, *in* SEP-97: Stanford Exploration Project, 343–351.

Schwab, M., 1998, Enhancement of discontinuities in seismic 3-D images using a Java estimation library: PhD thesis, Stanford University.

Schwab, M., C. Holden, and J. Claerbout, 1996, Revealing geological discontinuities by local plane wave suppression, *in* SEP-92: Stanford Exploration Project, 29–47.

Zhao, Y., 1999, Helix derivative and low-cut filters' spectral feature and application, *in* SEP-100: Stanford Exploration Project, 235–250.